# A Comparative Study of Gold Nanocubes, Octahedra, and Rhombic Dodecahedra as Highly Sensitive SERS Substrates

Hsin-Lun Wu, Huei-Ru Tsai, Yun-Ting Hung, Ka-Un Lao, Ching-Wen Liao, Pei-Ju Chung, Jer-Shing Huang, I-Chia Chen, and Michael H. Huang*

Department of Chemistry, National Tsing Hua University, Hsinchu 30013, Taiwan

Ⓢ *Supporting Information*

ABSTRACT: Gold nanocubes, octahedra, and rhombic dodecahedra with roughly two sets of particle sizes have been successfully synthesized via a seed-mediated growth approach. All six samples were analyzed for comparative surface-enhanced Raman scattering (SERS) activity. All of these Au nanostructures were found to yield strong enhancement at a thiophenol concentration of 10^{-7} M and are excellent SERS substrates. Rhombic dodecahedra with a rhombus edge length of 32 nm showed significantly better enhancement than the other samples and can reach a detection limit of 10^{-8} M. Simulations of the binding energies of thiophenol on the different faces of gold and electric near-field intensities of these nanocrystals have been performed to evaluate the experimental results. Superior SERS activity of these nanocrystals can be expected toward the detection of many other molecules.
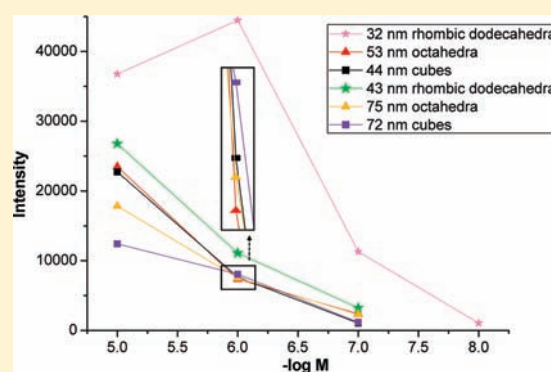
INTRODUCTION

Preparation of nanocrystals with excellent morphology control is necessary for demonstrations of their shape- and facet-dependent optical, catalytic, electrical, and surface properties.[1-5] Advances in the synthesis of polyhedral gold nanocrystals with well-defined shapes such as cubic, octahedral, rhombic dodecahedral, and icosahedral structures have been made recently.[6-13] Thus, it is now possible to examine their catalytic and surface properties if they are close in size and are synthesized under a similar reaction environment. An interesting and important topic to investigate is their relative sensitivity as surface-enhanced Raman scattering (SERS) substrates. Various different Au and Ag nano- and microstructures have been examined for their use as SERS substrates.[3,12,14-20] Octahedral Ag nanocrystals have been shown to outperform cuboctahedral and cubic Ag nanocrytals for trace arsenic detection via SERS spectroscopy.[3] However, cubic, octahedral, and rhombic dodecahedral Au nanocrystals bound respectively by only {100}, {111}, and {110} surfaces have not been compared for their relative SERS sensitivity. SERS activity is related to the large localized field enhancement such as the presence of sharp tips and is thus critically shape-dependent for nanoparticles. Molecular interactions with the various surface planes of Au nanocrystals can also affect the observed SERS intensity. In this study, we have taken Raman spectra of thiophenol in these Au nanocrystal solutions over a wide range of thiophenol concentrations to evaluate shape-dependent SERS activity of Au nanocrystals. The nanocrystals were synthesized using the procedure developed in our laboratory with similar reaction conditions. For each nanocrystal structure, two particle sizes have been used. These two particle sizes were chosen because they can be synthesized with good size uniformity. Binding energies of thiophenol on the different crystal faces were found to vary significantly and can partially explain the observed SERS results. Electric near-field simulations on the surface regions of the nanoparticles were performed to provide additional insights.

MATERIALS AND METHODS

Materials. Thiophenol (97%, AVOCADO), hydrogen tetrachloroaurate trihydrate ($HAuCl_4 \cdot 3H_2O$, 99.9%, Aldrich), cetyltrimethylammonium chloride (CTAC, 95%, TCI), sodium borohydride ($NaBH_4$, 98%, Aldrich), ascorbic acid (99.7%, Riedel-de-Haën), and sodium bromide (NaBr, UCW) were used without further purification. Ultrapure distilled and deionized water was used for all solution preparations. The procedure for making Au nanocubes and rhombic dodecahedra follows our reported method,[6] while the procedure described below for synthesizing Au octahedra is new.

Synthesis of Au Seed Particles. A volume of 10 mL of an aqueous solution containing 2.5×10^{-4} M $HAuCl_4$ and 0.10 M CTAC was prepared. Concurrently, 10 mL of 0.02 M ice-cold $NaBH_4$ solution was made. To the $HAuCl_4$ solution was added 0.45 mL of the $NaBH_4$ solution with stirring. The resulting solution turned brown immediately, indicating the formation of gold particles. The seed solution was aged for 1 h at 30 °C.

Synthesis of Smaller Au Nanocubes, Octahedra, and Rhombic Dodecahedra. Two vials were labeled A and B. A growth solution was prepared in each of the two vials. First, 0.32 g of CTAC
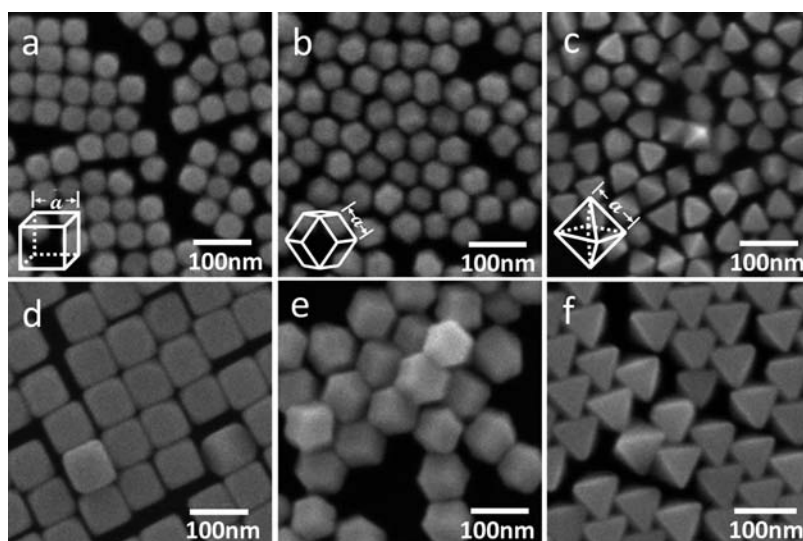
Figure 1. SEM images of (a, d) cubic, (b, e) rhombic dodecahedral, and (c, f) octahedral gold nanocrystals with edge lengths of (a) 44, (b) 32, (c) 53, (d) 72, (e) 43, and (f) 75 nm. Geometric models and edge lengths of these nanocrystals are also provided.

surfactant was added. The concentration of CTAC in the final solution was equal to 0.10 M. Depending on the morphology of gold nanocrystals to be synthesized, slightly different volumes of deionized water were added to each vial (i.e., 9.545 mL for rhombic dodecahedra, 9.605 mL for nanocubes, and 9.470 mL for octahedra). The vials were then kept in a water bath set at 30 °C. To both vials were added 250 μL of 0.01 M HAuCl$_4$ solution and 10 μL of 0.01 M NaBr for rhombic dodecahedra and nanocubes. For octahedra, 5 μL of 0.01 M KI was added instead of NaBr. Finally, 150, 90, and 220 μL of ascorbic acid was introduced for the synthesis of rhombic dodecahedra, nanocubes, and octahedra, respectively. The total solution volume in each vial was 10 mL. The solution color turned colorless after the addition of ascorbic acid, indicating the reduction of Au^{3+} to Au^{+} species. Next, 45 μL (for rhombic dodecahedra and nanocubes) or 55 μL (for octahedra) of the seed solution was added to the solution in vial A with shaking until the solution color turned light pink ($\sim$5 s). Then 45 μL (for rhombic dodecahedra and nanocubes) or 55 μL (for octahedra) of the solution in vial A was transferred to vial B with thorough mixing for $\sim$10 s. The solution in vial B was left undisturbed for 15 min for particle growth and centrifuged three times at 3000 rpm for 10 min (Hermle Z323 centrifuge). The particles were concentrated to a 1 mL solution.

Synthesis of Larger Au Rhombic Dodecahedra, Nanocubes, and Octahedra. The synthetic process is the same as that described above. To increase the particle size, one just needs to change the volumes of deionized water used to 9.565, 9.625, and 9.490 mL respectively for rhomic dodecahedra, nanocubes, and octahedra and change the volume of the seed solution added to the solution in vial A to 25 μL for rhombic dodecahedra and nanocubes or 35 μL for octahedra. The same volume should be transferred to vial B.

SERS Sample Prepration and Weighting Procedure. The aqueous Au nanocrystal solutions for SERS spectra were prepared by diluting 100 μL of the concentrated Au nanocrystal solutions to 1 mL with ethanol containing 1×10^{-5} to 1×10^{-8} M thiophenol. To determine the weight of nanocrystals used in a SERS experiment, the top solution after centrifugation of the synthesized nanoparticles to remove the surfactant was carefully withdrawn to avoid disturbance of the precipitate. Water was then added to disperse the precipitate and bring the total solution volume to 1 mL. This volume of nanocrystal solution was dried to obtain the particle weight using an analytical balance with precision to five digits after the decimal point. The actual nanocrystal weight used for the SERS experiment is 1/10 of the measured weight

since only 0.1 mL of the concentrated particle solution was transferred. Smaller nanocrystals are more likely than larger ones to be extracted during top solution withdrawal, so their measured weights may be slightly less than the synthesized amount.

Instrumentation. Scanning electron microscopy (SEM) characterization of the nanocrystals was performed using a JEOL JSM-7000F scanning electron microscope. To obtain SERS spectra, samples were excited with a He−Ne laser at 632.8 nm (Melles-Griot, 15 mW). The scattered light was collected at backscattering geometry and detected with a thermoelectric cooled CCD detector (Princeton Instrument).

Binding Energy Calculations. The gold surfaces for adsorption of thiophenol were modeled using gold clusters with 25 gold atoms distributed in two layers. The model of Au {111} and {110} surfaces was set up by arranging 16 and 9 gold atoms in the first and the second layer, respectively. The Au {100} surface was mimicked by 13 gold atoms in the first layer and 12 gold atoms in the second layer. All calculations were performed using the Gaussian 09 software package. Details of the computation methods used for the density function theory (DFT) calculations have been submitted elsewhere.

■ RESULTS AND DISCUSSION

The cubic and rhombic dodecahedral Au nanocrystals were synthesized following a seed-mediated growth approach.[6] Briefly, a gold seed particle solution was prepared first. A small volume of this solution was added to an aqueous growth solution containing cetyltrimethylammonium chloride (CTAC) surfactant, HAuCl$_4$, NaBr, and ascorbic acid. After mixing for $\sim$5 s, a small volume of this solution was added to another growth solution. The solution was left undisturbed for 15 min in a 30 °C water bath for nanocrystal growth. Use of the CTAC surfactant and the introduction of a small amount of NaBr in the growth solution are crucial to the formation of Au nanocrystals with systematic shape evolution from cubic to trisoctahedral and rhombic dodecahedral structures.

Figure 1 gives the SEM images of these Au nanocrystals. The nanoparticles are quite uniform in size and shape. Nanocubes with edge lengths of 44 and 72 nm were synthesized. For the rhombic dodecahedra, particles with approximate edge lengths of

8107

dx.doi.org/10.1021/ic200504n |*Inorg. Chem.* 2011, 50, 8106–8111
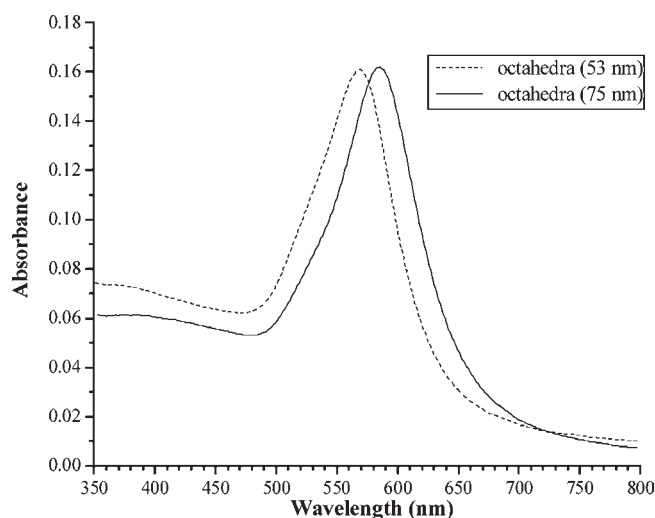
Figure 2. UV—vis absorption spectra of the octahedral Au nanocrystals with edge lengths of 53 and 75 nm.

Figure 3. SERS spectra of 1.0×10^{-7} M thiophenol in the cubic, octahedral, and rhombic dodecahedral Au nanocrystal solutions. Intensity of the band at 998 cm^{-1} is given for each sample. This band is used for all SERS comparison purposes in this work. The excitation wavelength is 632.8 nm.

32 and 43 nm (or opposite face-to-face distances of 52.3 and 70.2 nm) were produced. Edge lengths are used to indicate the particle sizes because these numbers are actually used in the electric near-field calculations of different nanocrystal shapes discussed later. Remarkably, octahedral Au nanocrystals can also be prepared using the same procedure by simply replacing NaBr with KI and adjusting the volumes of ascorbic acid and seed particle solution added. Monodisperse octahedral Au nanocryst-als with edge lengths of 53 and 75 nm (or opposite corner-to-corner distances of 74.2 and 105 nm) were produced by varying the volume of seed particle solution used. Their UV—vis absorption spectra show a single absorption band centered at 570 and 585 nm for the octahedral nanocrystals with respective edge lengths of 53 and 75 nm (see Figure 2). UV—vis absorption spectra of the nanocubes and rhombic dodecahedra are available in the Supporting Information.

Similar synthetic conditions and the same centrifugation process for facile surfactant removal used here means that a comparison of their SERS activity is more reliable. The same amount of concentrated nanocrystals was extracted in the pre-paration of SERS samples (i.e., 0.1 mL). The fresh nanocrystal solutions are dilute enough in the SERS samples that they are almost colorless. The particles are considered not aggregated. Surprisingly, SERS signals were obtained only at sufficiently low nanocrystal concentrations. Figure 3 displays the SERS spectra of 1.0×10^{-7} M thiophenol in cubic, octahedral, and rhombic dodecahedral Au nanocrystal solutions. The corresponding SERS spectra with thiophenol at concentrations of 1.0×10^{-5}, 1.0×10^{-6}, and 1.0×10^{-8} M are provided in the Supporting Information. The Raman band at 998 cm^{-1}, which is assigned to the C—C ring out-of-plane deformation and C—H out-of-plane bending of thiophenol, has been used as a reference band for all comparison purposes in this study.[21] This band has also been used for quantitative SERS intensity comparison of different metal surfaces.[22] The spectra show that Raman signals can still be recorded for all of the Au nanocrystal structures even at a very low thiophenol concentration of 1.0×10^{-7} M. This molecular concentration is already below or comparable to those typically used for the SERS measurements of silver nanostructures.[14,16,17] Considering that Ag surfaces are generally better SERS substrates
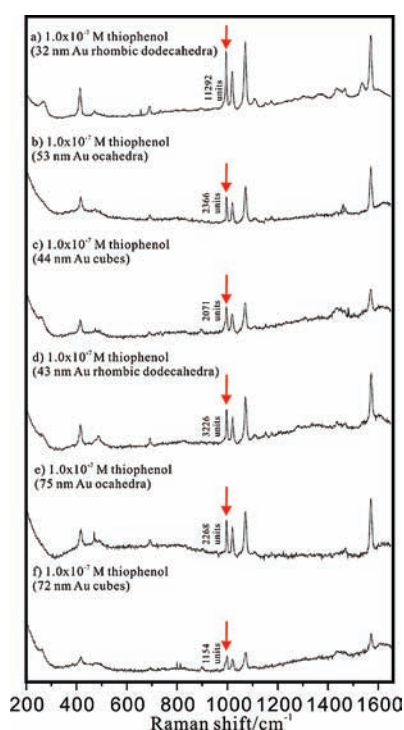
than the corresponding Au surfaces, the results indicate that Au nanocubes, octahedra, and rhombic dodecahedra can all serve as excellent SERS substrates. Since they represent three typical metal surfaces (i.e., {100}, {111}, and {110} faces), this may explain why various Au nanostructures have been reported to be SERS-active. The spectra reveal that rhombic dodecahedral Au nanocrystals are more sensitive than the cubic and octahedral Au nanocrystals with similar sizes and that the rhombic dodecahedra with an average edge length of 32 nm are the most sensitive toward the detection of thiophenol.

To see the whole picture of relative SERS activity of these Au nanostructures, intensities of the 998 cm^{-1} band from all of the spectra collected over the range of 1.0×10^{-5} to 1.0×10^{-8} M thiophenol are presented in Figure 4. Total surface-area-normal-ized SERS intensities of these nanocrystals for the band at 998 cm^{-1} are also provided to offer additional perspective. It is worth it to note that the total particle surface areas were derived from the weights of dried nanocrystal products synthesized; a loss of a tiny amount of nanoparticles during top solution extraction from the centrifuged precipitates may be more likely to happen for the smaller nanocrystals. Interpretation of the results shown in Figure 4b needs to take this factor into conside-ration. Rhombic dodecahedral Au nanocrystals show the best signal enhancement over the entire concentration range and are the best SERS substrates (see Figure 4a). In particular, the rhombic dodecahedra with an edge length of 32 nm display enormously strong enhancement compared to all other nano-structures, such that the SERS signal can still be observed even at a thiophenol concentration of 10^{-8} M. SERS signals were not mea-surable for the other Au nanostructures at this low thiophenol

8108

dx.doi.org/10.1021/ic200504n |*Inorg. Chem.* 2011, 50, 8106–8111
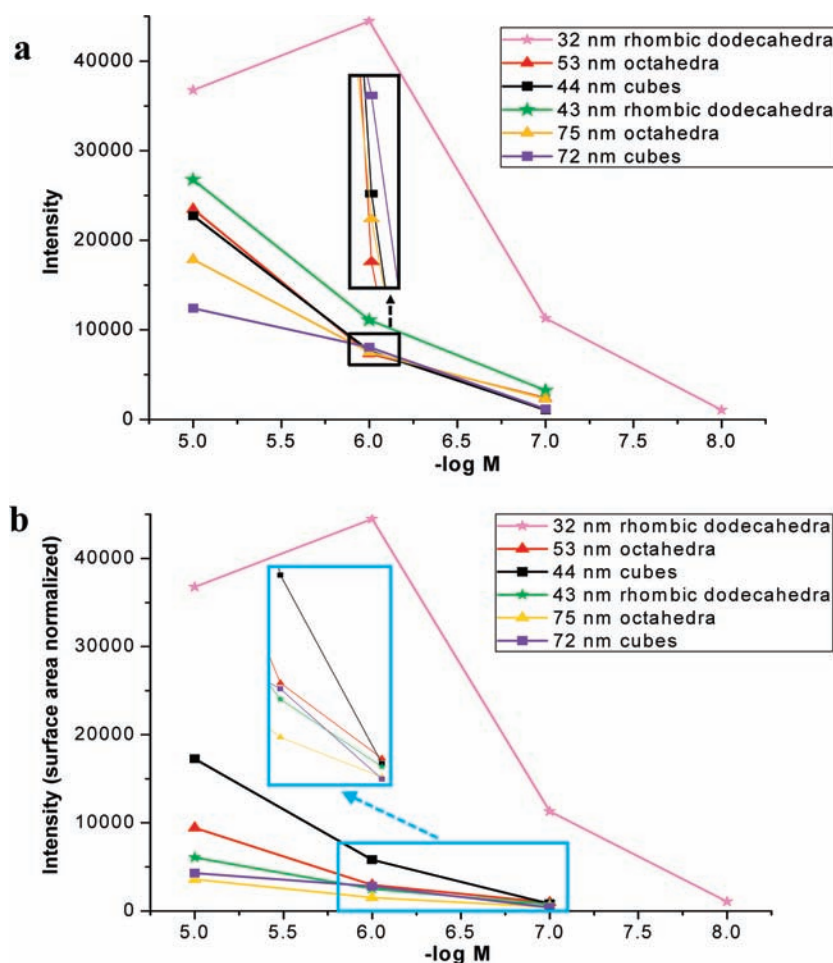
Figure 4. (a) A plot of the SERS intensities of the band at 998 cm^{-1} versus thiophenol concentrations in the Au nanocrystal solutions. Data points at a 1.0×10^{-6} M thiophenol concentration have been expanded to make their relative intensities visible. (b) A plot of the total particle surface-area-normalized intensities of the band at 998 cm^{-1} versus thiophenol concentrations in the Au nanocrystal solutions.

concentration. Interestingly, higher peak intensity at a lower molecular concentration is possible, as found for the 32 nm rhombic dodecahedra case. We found in separate experiments that peak intensity at 10^{-6} M can actually be somewhat higher than that measured at 10^{-5} M. The finding illustrates the value of successful preparation of rhombic dodecahedral Au nanocrystals with good particle size control, which have not been readily available until recently. The plot also shows that at a relatively high thiophenol concentration of 10^{-5} M, all other Au nano-structures are SERS-active with strong Raman intensities. At this molecular concentration, the Raman peak intensities measured for the smaller cubes and octahedra are substantially higher than those obtained for the corresponding structures with larger sizes. However, at a low thiophenol concentration of 10^{-6} M, cubes and octahedra of both sizes have similar peak intensities. Figure 4b also shows that smaller nanocrystals are generally more SERS-active and that rhombic dodecahedra give higher peak intensities than the other two particle shapes of similar sizes do at a thiophenol concentration of 10^{-5} M.

Octahedral Au nanocrystals have been shown to generate a strong polarized light-induced electric field at the corners.[9] Considering the sharp corners of octahedra and better field enhancement typically found at the nanocrystal tips, it was expected that octahedra should be the best and most sensitive

SERS substrates.[23] Corners of a cube also appear sharper than those of a rhombic dodecahedron. To explain the observations made in this study, electric near-field intensities of these nano-crystals upon laser excitation and chemical interactions of thiophenol on different gold surface planes are determined.

The SERS intensity can be expressed as

$$I_{SERS} = k \times P \times I^2 \times N \tag{1}$$

where k is a proportional constant including the information on the detection efficiency of the optical system, P is the polariz-ability of the molecules binding to the surface, I is the electric near-field intensity, and N is the average number of molecules binding to the metal surface that give SERS signals. The number of molecules binding to the nanoparticle surface, N, can be obtained from the following reaction (see Figure S5, Supporting Information):

$$thiophenol + surface\ Au\ atoms \overset{K}{\leftrightarrow} thiophenol@Au$$
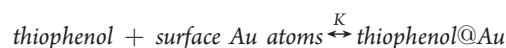
Knowing the equilibrium constant, the concentration of thio-phenol molecules, and the number density of surface Au atoms, we can rewrite N, or the number of thiophenol@Au, as:

$$N = K \times [thiophenol] \times [surface\ Au\ atoms] \tag{2}$$

Table 1. List of All of the Parameters for the Calculations of I_{SERS} for the Six Gold Nanocrystal Samples[a]

sample	I	$e^{E_b/RT}$	ρ_A (atoms/Å^2)	A_p (cm^2)	W_t (g)	V_p (cm^3)	$I^2 \cdot e^{E_b/RT} \cdot \rho_A \cdot A_p \cdot W_t/V_p$
CB44	1.71895	6.8009×10^{12}	0.12956	1.16×10^{-10}	0.0000175	8.52×10^{-17}	6.21×10^{13}
CB72	5.57962	6.8009×10^{12}	0.12956	3.11×10^{-10}	0.0000628	3.73×10^{-16}	1.44×10^{15}
OH53	2.00149	476184.747	0.15677	9.73×10^{-11}	0.0000326	7.02×10^{-17}	1.35×10^{7}
OH75	3.96949	476184.747	0.15677	1.95×10^{-10}	0.0000924	1.99×10^{-16}	1.06×10^{8}
RD32	2.56729	3.193×10^{24}	0.09378	1.16×10^{-10}	0.0000158	1.01×10^{-16}	3.58×10^{25}
RD43	3.3373	3.193×10^{24}	0.09378	2.09×10^{-10}	0.0000936	2.45×10^{-16}	2.67×10^{26}

[a] CB, OH, and RD stand for cubes, octahedra, and rhombic dodecahedra. Sample labels also include their edge lengths. I is the calculated electric near-field intensity of a single nanoparticle. ρ_A is the area density of gold atoms on the surface. ρ_A = atoms per unit cell/area of unit cell. A_p is the surface area per particle. W_t is the weight of the gold nanocrystals used for the SERS experiment. V_p is the volume per particle.

In the case of a very dilute thiophenol concentration, the equilibrium constant can be expressed as a function of the binding energy (E_b) determined by considering the interactions between the whole thiophenol molecule and 25 gold atoms distributed in two layers (see the Supporting Information for detail):

$$K = e^{E_b/RT} \tag{3}$$

where R is the gas constant and T is the reaction temperature in Kelvin (298 K for room temperature). The assumption may be valid for this work since both thiophenol and gold particle concentrations are very low.

We obtained binding energies of thiophenol on the {111}, {100}, and {110} surface planes of gold using DFT calculations (see the Supporting Information). The binding energies between thiophenol and the gold {111}, {100}, and {110} surface planes are 7.742, 17.498, and 33.413 kcal/mol, respectively. Because of the much larger binding energy of thiophenol on the {110} plane of gold, K is many orders of magnitude larger than those on the {111} and {100} planes. Consequently, N is very large for the {110} surface plane, and I_{SERS} should also become very large. This finding agrees with the experimental observation that rhombic dodecahedral gold nanocrystals give the highest SERS intensity and sensitivity.

The number of the surface gold atoms can be quantitatively calculated from the area density of gold atoms on the surface (ρ_A), the surface area per particle (A_p), and the total number of nanoparticles in the suspension (n_p).

[surface Au atoms], or the total number of surface Au atoms

$$= \rho_A \times A_p \times n_p \tag{4}$$

Here, the area density (ρ_A) of the Au atoms is calculated from its bond length and atom-to-atom distance. We used the smallest two-dimensional unit cells of Au to determine the number of atoms within the unit cell surface areas (see the Supporting Information). The surface area per particle (A_p) is estimated using the morphology and dimensions measured from the SEM images. As for the number of nanoparticles in the suspension (n_p), we obtained an estimated value by weighting the dried nanocrystals and dividing the total weight (W_t) by the weight of a single particle, which is the product of the crystal volume density (D_v = 19.3 g/cm^3) and the volume per particle (V_p).

$$[surface \; Au \; atoms] = \rho_A \times A_p \times W_t/(D_v \times V_p) \tag{5}$$

The electric near-field intensity is estimated by finite-difference time-domain simulations (FDTD solutions V. 6.5, Lumerical

Solutions Inc., Canada) using real particle dimensions obtained from the representative SEM images (see Figure 1). Details of the simulation procedure are available in the Supporting Information. From eqs 1, 2, 3, and 5, the SERS intensity can be expressed as

$$I_{SERS} = k \times P \times I^2 \times e^{E_b/RT} \times [thiophenol] \times \rho_A$$
$$\times A_p \times W_t/(D_v \times V_p) \tag{6}$$

Since we have not observed any shift of the Raman peaks, the polarizability P is a constant for the bands at 998 cm^{-1}. The proportional constant k taking into account the efficiency of the optical system is also a constant since all experimental conditions are kept the same for all three particles. Finally, the concentration of thiophenol used in the experiment is also the same for all three nanoparticle structures (e.g., at a thiophenol concentration of 1.0×10^{-7} M). Therefore, the intensity of the SERS peak is only proportional to I^2 and N and can be expressed as

$$I_{SERS} \propto I^2 \times e^{E_b/RT} \times \rho_A \times A_p \times W_t/V_p \tag{7}$$

The signal coming from the free diffusing molecules is not significant here since the electric near field is typically confined within a thin layer of less than 100 nm, and the concentration is so dilute that the number of molecules within the layer is negligible. Table 1 lists all the parameters in eq 7.

From the electric near-field intensities, I, one can see that for bigger gold nanocrystals the values of I for a cube and octahedron are larger than that for a rhombic dodecahedron. Cubes with an edge length of 72 nm were found to have the largest I value. The results are consistent with the structural analysis that cubes and octahedra with sharper corners are likely better SERS substrates. Interestingly, I values for the smaller nanocrystals indicate that rhombic dodecahedra with an edge length of 32 nm have the largest electric near-field intensity. The results partially account for the experimental observation of these nanocrystals as the best and most sensitive SERS substrates. Products of all of the parameters in eq 7 also agree with experimental results that rhombic dodecahedra are the best SERS substrates. Of course, the main factor contributing to the large I_{SERS} is the large binding energy of thiophenol on the {110} surface plane of gold. Although the values of products of eq 7 differ quite substantially for the three nanocrystal morphologies as a result of large differences in the binding energies, the calculations qualitatively explain the SERS data. To obtain more realistic values proportional to experimentally measured I_{SERS}, instead of using the binding energy, one needs to consider the actual number of thiophenols binding to the gold nanoparticle surface, which include the concentration and maximum coverage of the molecules on the gold surface. However, the present treatment illustrates

that in addition to electric near-field intensity as a major consideration for SERS enhancement, molecular binding energy or strength of molecular interactions with different metal surface planes may also be important to the SERS intensities of nanocrystals.

■ CONCLUSIONS

In summary, gold nanocubes, octahedra, and rhombic dodecahedra with two different sizes have been synthesized by a seed-mediated growth approach. They were examined for their comparative SERS activity. All of these nanocrystals can serve as sensitive SERS substrates, but rhombic dodecahedra with an edge length of 32 nm were found to give the strongest signal enhancement with the lowest detection limit of thiophenol down to 10^{-8} M. Binding energy and electric near-field intensity calculations have been performed to evaluate the experimental results. It is expected that rhombic dodecahedral gold nanocrystals should also serve as superior SERS substrates for the detection of a wide variety of molecules.

■ ASSOCIATED CONTENT

ⓢ Supporting Information. UV–vis absorption spectra of Au nanocubes and rhombic dodecahedra, additional SERS spectra, most stable structures of thiophenol on different gold surfaces, area density and total particle number calculations, and electric near-field intensity simulation methods. This material is available free of charge via the Internet at http://pubs.acs.org.

■ AUTHOR INFORMATION

Corresponding Author
*E-mail: hyhuang@mx.nthu.edu.tw.

■ ACKNOWLEDGMENT

■ REFERENCES

(1) Bratlie, K. M.; Lee, H.; Komvopoulos, K.; Yang, P.; Somorjai, G. A. *Nano Lett.* **2007**, *7*, 3097.

(2) (a) Ho, J.-Y.; Huang, M. H. *J. Phys. Chem. C* **2009**, *113*, 14159. (b) Lyu, L.-M.; Wang, W.-C.; Huang, M. H. *Chem.—Eur. J.* **2010**, *16*, 14167. (c) Kuo, C.-H.; Yang, Y.-C.; Gwo, S.; Huang, M. H. *J. Am. Chem. Soc.* **2011**, *133*, 1052. (d) Wang, W.-C.; Lyu, L.-M.; Huang, M. H. *Chem. Mater.* **2011**, *23*, 2677.

(3) Mulvihill, M.; Tao, A.; Benjauthrit, K.; Arnold, J.; Yang, P. *Angew. Chem., Int. Ed.* **2008**, *47*, 6456.

(4) Komanicky, V.; Iddir, H.; Chang, K.-C.; Menzel, A.; Karapetrov, G.; Hennessy, D.; Zapol, P.; Yoo, H. *J. Am. Chem. Soc.* **2009**, *131*, 5732.

(5) Ringe, E.; McMahon, J. M.; Sohn, K.; Cobley, C.; Xia, Y.; Huang, J.; Schatz, G. C.; Marks, L. D.; Van Duyne, R. P. *J. Phys. Chem. C* **2010**, *114*, 12511.

(6) Wu, H.-L.; Kuo, C.-H.; Huang, M. H. *Langmuir* **2010**, *26*, 12307.

(7) (a) Seo, D.; Park, J. C.; Song, H. *J. Am. Chem. Soc.* **2006**, *128*, 14863. (b) Seo, D.; Yoo, C. I.; Park, J. C.; Park, S. M.; Ryu, S.; Song, H. *Angew. Chem., Int. Ed.* **2008**, *47*, 763.

(8) Chang, C.-C.; Wu, H.-L.; Kuo, C.-H.; Huang, M. H. *Chem. Mater.* **2008**, *20*, 7570.

(9) Li, C.; Shuford, K. L.; Park, Q.-H.; Cai, W.; Li, Y.; Lee, E. J.; Cho, S. O. *Angew. Chem., Int. Ed.* **2007**, *46*, 3264.

(10) Jeong, G. H.; Kim, M.; Lee, Y. W.; Choi, W.; Oh, W. T.; Park, Q.-H.; Han, S. W. *J. Am. Chem. Soc.* **2009**, *131*, 1672.

(11) Kim, D. Y.; Im, S. H.; Park, O. O.; Lim, Y. T. *CrystEngComm* **2010**, *12*, 116.

(12) Kwon, K.; Lee, K. Y.; Lee, Y. W.; Kim, M.; Heo, J.; Ahn, S. J.; Han, S. W. *J. Phys. Chem. C* **2007**, *111*, 1161.

(13) Xu, J.; Li, S.; Weng, J.; Wang, X.; Zhou, Z.; Yang, K.; Liu, M.; Chen, X.; Cui, Q.; Cao, M.; Zhang, Q. *Adv. Funct. Mater.* **2008**, *18*, 277.

(14) Zhang, Q.; Li, W.; Moran, C.; Zeng, J.; Chen, J.; Wen, L.-P.; Xia, Y. *J. Am. Chem. Soc.* **2010**, *132*, 11372.

(15) Mulvihill, M. J.; Ling, X. Y.; Henzie, J.; Yang, P. *J. Am. Chem. Soc.* **2010**, *132*, 268.

(16) Gutés, A.; Carraro, C.; Maboudian, R. *J. Am. Chem. Soc.* **2010**, *132*, 1476.

(17) Zhang, J.; Li, X.; Sun, X.; Li, Y. *J. Phys. Chem. B* **2005**, *109*, 12544.

(18) Orendorff, C. J.; Gole, A.; Sau, T. K.; Murphy., C. J. *Anal. Chem.* **2005**, *77*, 3261.

(19) Camden, J. P.; Dieringer, J. A.; Zhao, J.; Van Duyne, R. P. *Acc. Chem. Res.* **2008**, *41*, 1653.

(20) Barbosa, S.; Agrawal, A.; Rodríguez-Lorenzo, L.; Pastoriza-Santos, I.; Alvarez-Puebla, R. A.; Kornowski, A.; Weller, H.; Liz-Marzán, L. M. *Langmuir* **2010**, *26*, 14943.

(21) Xu, X.-Y.; Li, S.-J.; Wu, D.-Y.; Gu, R.-A. *Acta Chim. Sinica* **2007**, *65*, 1095.

(22) Taylor, C. E.; Pemberton, J. E.; Goodman, G. G.; Schoenfisch, M. H. *Appl. Spectrosc.* **1999**, *53*, 1212.

(23) Rycenga, M.; Kim, M. H.; Camargo, P. H. C.; Cobley, C.; Li, Z.-Y.; Xia, Y. *J. Phys. Chem. A* **2009**, *113*, 3932.

8111

dx.doi.org/10.1021/ic200504n |*Inorg. Chem.* 2011, 50, 8106–8111